Performance Analysis of Coherent and Noncoherent Modulation under I/Q Imbalance

Bassant Selim, *Member, IEEE*, Sami Muhaidat, *Senior Member, IEEE*,
Paschalis C. Sofotasios, *Senior Member, IEEE*, Bayan S. Sharif, *Senior Member, IEEE*,
Thanos Stouraitis, *Fellow, IEEE*, George K. Karagiannidis, *Fellow, IEEE* and Naofal Al-Dhahir, *Fellow, IEEE*

***Abstract*—In-phase/quadrature-phase Imbalance (IQI) is considered a major performance-limiting impairment in direct-conversion transceivers. In this paper, we quantify the effects of IQI on the performance of different modulation schemes under multipath fading channels. In particular, a general framework for the analysis of the symbol error rate (SER) of coherent phase shift keying, noncoherent differential phase shift keying and noncoherent frequency shift keying under IQI effects is derived. In more details, the moment generating function of the signal-to-interference-plus-noise-ratio is first derived for both point-to-point and multi-antenna receiver based single-carrier and multi-carrier systems, encountering transmitter (TX) IQI only, receiver (RX) IQI only and joint TX/RX IQI. Capitalizing on this, we derive analytic expressions for the SER of the aforementioned modulation schemes, for both point to point and multiple-antenna systems, and provide useful insights into the dependence of IQI on the system parameters. We further demonstrate that while in some cases IQI can cause a negligible degradation of the SER performance, in other cases, this impairment is more pronounced; as a result, it should be compensated in order to achieve a reliable communication link.**

***Index Terms*—I/Q imbalance, coherent detection, noncoherent detection, RF impairments, symbol error rate.**

I. Introduction

The emergence of the Internet of Things (IoT) along with the ever-increasing demands of the mobile Internet impose high spectral efficiency, low latency and massive connectivity requirements on fifth generation (5G) wireless networks and beyond. Accordingly, next-generation wireless communication systems are expected to support heterogeneous devices for various standards and services with particularly high throughput and low latency requirements. This calls for flexible and software reconfigurable transceivers that are capable of supporting the desired quality of service demands. To this end, direct conversion transceivers have attracted considerable attention owing to their suitability for higher levels of integration and their reduced cost and power consumption since they require neither external intermediate frequency filters nor image rejection filters. However, in practical communication scenarios, direct-conversion transceiver architectures inevitably suffer from radio-frequency (RF) front-end related impairments such as phase noise, DC offset and in-phase/quadrature-phase imbalances (IQI), which limit the overall system performance [1]. In this context, IQI, which refers to the amplitude and phase mismatch between the I and Q branches of a transceiver, leads to imperfect image rejection, which results in performance degradation of both conventional and emerging communication systems [2], [3]. In ideal scenarios, the I and Q branches of a mixer have equal amplitude and a phase shift of $90°$, providing an infinite attenuation of the image band; however, in practice, direct-conversion transceivers are sensitive to certain analog front-end related impairments that introduce errors in the phase shift as well as mismatches between the amplitudes of the I and Q branches which corrupt the down-converted signal constellation, thereby increasing the corresponding error rate [2].

It is already established that depending on the receiver's (RX) ability to exploit knowledge of the carrier's phase to detect the signals, the detection can be classified into coherent and noncoherent [3]. Coherent information detection requires full knowledge of the channel state information (CSI) at the receiver. On the other hand, noncoherent detection has been proposed as an efficient technique particularly for low-power wireless systems such as wireless sensor networks and relay networks [4]. It has been demonstrated that, particularly in the context of massive multi-input multi-output (MIMO) systems, the pilot overhead could exhaust needed resources and, hence, noncoherent systems could lead to a better spectral efficiency [5]. Another main advantage of these schemes stems from the fact that they reduce the receiver complexity since they eliminate the need for channel estimation and tracking [6], [7]. However, this comes at the cost of higher error rate or lower spectral efficiency; as a result, selecting the most suitable modulation scheme depends on the considered application.

A. Related Work

I/Q signal processing is widely utilized in modern communication transceivers which gives rise to the problem of matching the amplitudes and phases of the branches, resulting in an interference from the image signal. Motivated by this

B. Selim was with the Department of Electrical Engineering and Computer Science, Khalifa University, Abu Dhabi, UAE. She is now is with the Electrical Engineering Department, ETS, University of Quebec, Montreal, QC H3C 1K3, Canada (email:bassant.selim.1@ens.etsmtl.ca).

S. Muhaidat, P. C. Sofotasios, B. Sharif and T. Stouraitis are with the Department of Electrical Engineering and Computer Science, Khalifa University, Abu Dhabi, UAE (e-mails: {muhaidat, p.sofotasios}@ieee.org and {bayan.sharif; thanos.stouraitis}@ku.ac.ae).

G. K. Karagiannidis is with the Department of Electrical and Computer Engineering, Aristotle University of Thessaloniki, 54124 Thessaloniki, Greece (e-mail: geokarag@auth.gr).

N. Al-Dhahir is with the Department of Electrical Engineering, University of Texas at Dallas, TX 75080 Dallas, USA (e-mail: aldhahir@utdallas.edu).

This paper was presented in part at the IEEE 87th Vehicular Technology Conference (VTC Spring), Porto, 2018.

practical concern, several recent works have proposed to model, mitigate or even exploit IQI, see [8] and the references therein. In [9], the SEP of M-ary phase shift keying (PSK) under IQI was investigated for Gaussian channels. Assuming differential quadrature phase shift keying (DQPSK) and Rayleigh fading, the bit error rate (BER) under IQI was derived for single-carrier systems in [10] and for both single-carrier and multi-carrier systems in [11]. Moreover, in [12], assuming single-carrier modulation, the effects of IQI on the SER of different coherent and noncoherent modulations was investigated. Under the assumption of IQI at the receiver only, the SINR probability distribution function (PDF) of generalized frequency division multiplexing under Weibull fading channels was derived and the average symbol error rate (SER) of M-ary quadrature amplitude modulation ($M-$QAM) was formulated in [13]. Similarly, for M-QAM modulation and Rayleigh fading channels, the error performance of multi-carrier systems and OFDM systems was investigated in [14]–[16] and [17], respectively. For the case of N*Nakagami-m fading conditions, the authors in [18] quantified the effects of IQI on the outage probability of both single-carrier and multi-carrier systems. Moreover, in [19]–[22], the authors analyzed the effects of IQI on the outage performance of non-orthogonal multiple access. IQI has also been studied in half-duplex and full duplex amplify-and-forward and decode-and-forward cooperative systems [23]–[26], two-way relay systems and multi-antenna systems [27]–[34],as well as cognitive radio systems [35]. Finally, the effects of IQI on uplink transmission have been analyzed in the context of massive multi-user MIMO in [36].

B. Contribution

To our best knowledge, the effects of RF impairments in noncoherent systems have been overlooked in the open literature so far, apart from some sporadic results [37]. In addition, the existing results on coherent detection are largely limited to non-holistic scenarios, and do not provide a comprehensive treatment of IQI in single and multi-carrier coherent systems. Motivated by this fact, in this work we extend our work in [12] and investigate the performance of single-carrier and multi-carrier based coherent and noncoherent systems under IQI. In particular, we derive the SINR moment generating functions (MGFs) of I/Q impaired systems, which are subsequently utilized to derive the SER expressions of $M-$PSK, M-QAM, $M-$DPSK and M-ary frequency shift keying ($M-$FSK) constellations for both point-to-point and multiple antenna systems. This also allows a comparison between the different systems under IQI, which is crucial in in the selection of the most appropriate technique for the considered system. In addition, the effect of IQI will be quantified in maximal ratio combining (MRC) based receivers, which require amplitude and phase knowledge and thus, not accounting IQI effects will ultimately turn out to be rather detrimental.

The main objective of this paper is to develop a general framework for the comprehensive analysis of coherent and noncoherent modulation schemes under different IQI scenarios. To this end, we consider both single-carrier and multi-carrier systems where, following the MGF approach, we quantify the effects of TX IQI, RX IQI and joint TX/RX IQI on *M*-PSK, *M*-DPSK and *M*-FSK constellations over multipath fading channels. In more details, the main contributions of this work are summarized as follows:

- We derive novel analytic expressions for the SINR PDF and the cumulative distribution function (CDF) for single-carrier systems over Rayleigh fading channels with TX and/or RX IQI along with a novel generalized closed form expression for the corresponding SINR MGF.
- We derive novel closed form expressions for the SINR PDF, CDF and MGF for the case of multi-carrier systems over Rayleigh fading channels with TX and/or RX IQI.
- We extend our results and derive the MGF of L-branch MRC receivers under the considered diffreent IQI scenarios.
- We derive the MGF for a differential Alamouti Space-Time Block Codes (STBC)-OFDM system under joint TX/RX IQI.
- Using the derived MGFs, we derive the corresponding SER expressions for the cases of *M*-PSK, *M*-DPSK and *M*-FSK constellations.

To the best of the authors' knowledge, the offered results have not been previously reported in the open technical literature.

C. Organization and Notations

The remainder of this paper is organized as follows: Section II provides a brief overview of the considered modulation schemes. In Sections III and IV, the SINR PDF, CDF and MGF are derived for single-carrier and multi-carrier systems with IQI, respectively. In addition, Section V presents the SER of *M*-PSK, *M*-DPSK and *M*-FSK under IQI. The extension to the multiple antenna case is given in Section VI, whereas the corresponding numerical results and discussions are provided in Section VII. Finally, closing remarks are given in Section VIII.

Notations: Unless otherwise stated, $(\cdot)^*$ denotes conjugation and $j=\sqrt{-1}$. The operators $\mathbb{E}[\cdot]$ and $|\cdot|$ denote statistical expectation and absolute value operations, respectively. Also, $f_X(x)$ and $F_X(x)$ denote the PDF and CDF of X, respectively while $\mathcal{M}_X(s)$ is the MGF associated with X. Finally, the subscripts t/r denote the up/down-conversion process at the TX/RX, respectively.

II. System model

We assume that a signal, s, is transmitted over a wireless channel, h, which follows a Rayleigh distribution and is subject to additive white Gaussian noise (AWGN), n. Assuming that the TX/RX are equipped with a single antenna, we first revisit briefly the signal model for the considered *M*-ary PSK, DPSK and FSK modulation schemes.

A. Coherent Detection of M-PSK Symbols

Assuming *M*-PSK modulation, it is recalled that

$$\theta_m = \frac{(2m-1)\,\pi}{M}, \qquad m=1,2,\ldots,M \tag{1}$$

Hence, the complex baseband signal at the transmitter in the l^{th} symbol interval is given by

$$s[l] = A_c \exp\left(j\theta[l]\right) \tag{2}$$

where $\theta[l]$ is the information phase in the l^{th} symbol. Assuming that the receiver has perfect knowledge of the CSI as well as carrier phase and frequency, the complex baseband signal at the receiver is represented as

$$x[l] = A_c \exp\left(j\theta[l]\right) + n[l]. \tag{3}$$

B. Noncoherent Detection of M-DPSK Symbols

Assuming M-ary DPSK modulation, the information phase in (1) is modulated on the carrier as the difference between two adjacent transmitted phases. Considering that the channel is slowly varying and remains constant over two consecutive symbols, the receiver takes the difference of two adjacent phases to reach a decision on the information phase without knowledge of the carrier phase and channel state [38]. In this context, the information phases $\Delta\theta[l]$ are first differentially encoded to a set of phases as follows:

$$\theta[l] = \left(\theta[l-1] + \Delta\theta[l]\right) \bmod 2\pi \tag{4}$$

where $\Delta\theta_m = (2m-1)\pi/M$, $m = 1, ..., M$ and $\Delta\theta[l]$ is the information phase in the l^{th} symbol interval. The modulated symbol $s[l]$ is then obtained by applying a phase offset to the previous symbol $s[l-1]$, namely,

$$s[l] = s[l-1] \exp\left(j\theta[l]\right) \tag{5}$$

where $s[1] = 1$. Similarly, the decision variable is obtained from the phase difference between two consecutive received symbols as follows

$$\widehat{s}[l] = r^*[l-1]r[l]. \tag{6}$$

C. Noncoherent Detection of M-FSK Symbols

Assuming *M*-FSK modulation, the M information frequencies are given by

$$f_m = (2m - 1 - M)\,\Delta f, \qquad m = 1, 2, \ldots, M \tag{7}$$

and thus the l^{th} complex baseband symbol at the transmitter is given by

$$s[l] = A_c \exp\left(j2\pi f[l]\right). \tag{8}$$

The decision variable at the receiver is then obtained by multiplying the received signal by the set of complex sinusoids $\exp\left(j2\pi f_m\right)$, $m = 1, 2, ..., M$ and passing them through M matched filters. For orthogonal signals, the frequency spacing is chosen as $\Delta f = N/T_s$, where T_s is the symbol period and N is an integer.

III. MGF of the Received SINR with IQI in Single-Carrier Systems

Single-carrier modulation is receiving increasing attention due to its robustness towards RF impairments compared to multi-carrier modulation; see [39] and the references therein. Hence, it is considered more suitable for low complexity and low power applications. In what follows, assuming that both the transmitter and receiver are equipped with a single antenna, we derive unified closed form expressions for the SINR PDF, CDF and MGF of single-carrier systems over flat fading Rayleigh channel in the presence of IQI.

At the receiver RF front end, the received bandpass signal undergoes various processing stages including filtering, amplification, and analog I/Q demodulation (down-conversion) to baseband and sampling. Assuming an ideal RF front end, the baseband equivalent received signal is represented as

$$r_{\text{id}} = hs + n \tag{9}$$

where the index l is dropped for notational convenience. Moreover, $h \sim \mathcal{CN}(0,1)$ denotes the channel coefficient and $n \sim \mathcal{CN}(0, N_0)$ is the circularly symmetric complex AWGN signal. The instantaneous signal to noise ratio (SNR) per symbol at the receiver input is given by

$$\gamma_{\text{id}} = \frac{E_s}{N_0} |h|^2 \tag{10}$$

where E_s is the energy per transmitted symbol. It is assumed that the RF subcarriers are up/down converted to the baseband by direct conversion architectures, while we assume frequency-independent IQI caused by the gain and phase mismatches of the I and Q mixers; however, the extension to frequency-dependent IQI is straightforward, following the approach in [40], [41]. In this context, the time-domain baseband representation of the IQI impaired signal is given by [42]

$$g_{\text{IQI}} = \mu_{t/r} g_{\text{id}} + \nu_{t/r} g_{\text{id}}^* \tag{11}$$

where g_{id} is the baseband IQI-free signal and g_{id}^* is due to IQI. In addition, the corresponding IQI coefficients $\mu_{t/r}$ and $\nu_{t/r}$ are given by

$$\mu_t = \frac{1}{2}\left(1 + \epsilon_t \exp\left(j\phi_t\right)\right), \tag{12}$$

$$\nu_t = \frac{1}{2}\left(1 - \epsilon_t \exp\left(-j\phi_t\right)\right), \tag{13}$$

$$\mu_r = \frac{1}{2}\left(1 + \epsilon_r \exp\left(-j\phi_r\right)\right), \tag{14}$$

and

$$\nu_r = \frac{1}{2}\left(1 - \epsilon_r \exp\left(j\phi_r\right)\right) \tag{15}$$

where $\epsilon_{t/r}$ and $\phi_{t/r}$ denote the TX/RX amplitude and phase mismatch levels, respectively. It is noted that for ideal RF front-ends, $\phi_{t/r} = 0^\circ$ and $\epsilon_{t/r} = 1$, which implies that $\mu_{t/r} = 1$ and $\nu_{t/r} = 0$. Moreover, the TX/RX image rejection ratio (IRR), which determines the amount of attenuation of the image frequency band, is given by

$$\text{IRR}_{t/r} = \frac{\left|\mu_{t/r}\right|^2}{\left|\nu_{t/r}\right|^2}. \tag{16}$$

A. Received SINR Under IQI

- *TX IQI and ideal RX:* This case assumes that the RX RF front-end is ideal, while the TX experiences IQI. In this case, the instantaneous SINR per symbol at the input of the receiver is given by [18]

$$\gamma_{\text{IQI}} = \frac{|\mu_t|^2}{|\nu_t|^2 + \frac{1}{\gamma_{\text{id}}}}. \tag{17}$$

- *RX IQI and ideal TX:* This case assumes that the TX RF front-end is ideal, while the RX is subject to IQI. Hence, at the RX input, the instantaneous SINR per symbol is expressed as [18]

$$\gamma_{\text{IQI}} = \frac{|\mu_r|^2}{|\nu_r|^2 + \frac{\Lambda}{\gamma_{\text{id}}}}. \tag{18}$$

  where $\Lambda = |\mu_r|^2 + |\nu_r|^2$.
- *Joint TX/RX IQI:* This case assumes that both TX and RX are impaired by IQI and the SINR can be approximated as [18]

$$\gamma_{\text{IQI}} \approx \frac{|\xi_{11}|^2 + |\xi_{22}|^2}{|\xi_{12}|^2 + |\xi_{21}|^2 + \frac{\Lambda}{\gamma_{\text{id}}}} \tag{19}$$

where $\xi_{11} = \mu_r\mu_t$, $\xi_{22} = \nu_r\nu_t^*$, $\xi_{12} = \mu_r\nu_t$, and $\xi_{21} = \nu_r\mu_t^*$.

B. SINR Distribution

From (17), (18) and (19), the SINR of single-carrier systems in the presence of IQI can be expressed as

$$\gamma_{\text{IQI}} = \frac{\alpha}{\beta + \frac{A}{\gamma_{\text{id}}}} \tag{20}$$

where the parameters α, β, and A are given in Table I.

TABLE I: Single-carrier systems impaired by IQI parameters

	α	β	A
TX IQI	$\lvert\mu_t\rvert^2$	$\lvert\nu_t\rvert^2$	1
RX IQI	$\lvert\mu_r\rvert^2$	$\lvert\nu_r\rvert^2$	Λ
Joint TX/RX IQI	$\lvert\xi_{11}\rvert^2 + \lvert\xi_{22}\rvert^2$	$\lvert\xi_{12}\rvert^2 + \lvert\xi_{21}\rvert^2$	Λ

Hence, the CDF of γ_{IQI} is obtained as

$$F_{\gamma_{IQI}}(x) = F_{\gamma_{id}}\left(\frac{A}{\frac{\alpha}{x} - \beta}\right) \tag{21}$$

where γ_{id} is the IQI free SNR, which follows an exponential distribution. Hence, assuming TX and/or RX IQI, the corresponding SINR CDF is given by

$$F_{\gamma_{\text{IQI}}}(x) = 1 - \exp\left(-\frac{A}{\overline{\gamma}\left(\frac{\alpha}{x} - \beta\right)}\right), \qquad 0 \le x \le \frac{\alpha}{\beta} \tag{22}$$

where $\overline{\gamma} = E_s/N_0$ is the average SNR. Given that $f_{\gamma_{\text{IQI}}}(x) = \frac{\mathrm{d}}{\mathrm{d}x}F_{\gamma_{\text{IQI}}}(x)$, the SINR PDF, in the presence of IQI, is given by

$$f_{\gamma_{\text{IQI}}}(x) = \frac{\alpha A \exp\left(-\frac{A}{\overline{\gamma}\left(\frac{\alpha}{x} - \beta\right)}\right)}{\overline{\gamma}\left(\alpha - x\beta\right)^2} \tag{23}$$

which is valid for $0 \le x \le \frac{\alpha}{\beta}$.

C. Moment Generating Function

The MGF is an important statistical metric and constitutes a convenient tool in digital communication systems over fading channels [38]. In what follows, we derive a generalized closed form expression for the SINR MGF of single-carrier systems in the presence of IQI, which will be particularly useful in the subsequent analysis.

Proposition 1. *For single-carrier systems impaired by IQI, the MGF of the instantaneous fading SINR is given by*

$$\mathcal{M}_{\gamma_{\text{IQI}}}(s) = \exp\left(\frac{\alpha}{\beta}s + \frac{A}{\beta\overline{\gamma}}\right)\Gamma\left(1, \frac{A}{\overline{\gamma}\beta}; \frac{s\alpha A}{\beta^2\overline{\gamma}}\right) \tag{24}$$

where $\Gamma(\alpha, x; b) = \int_x^\infty t^{\alpha-1}\exp\left(-t - \frac{b}{t}\right)\mathrm{d}t$ *denotes the extended upper incomplete Gamma function [43].*

Proof. The proof is provided in Appendix A □

IV. Multi-Carrier Systems MGF of the Received SINR with IQI

It is recalled that multi-carrier systems divide the signal bandwidth among K subcarriers, which provides several advantages including enhanced robustness against multipath fading. Long-Term Evolution (LTE) employs orthogonal frequency division multiplexing (OFDM) in the downlink. In this subsection, we derive the SINR PDF, CDF and MGF of multi-carrier systems over frequency selective channels in the presence of IQI. We assume that the RF subcarriers are down converted to the baseband by direct conversion. We also denote the set of signals as $S = \{-\frac{K}{2}, \ldots, -1, 1, \ldots, \frac{K}{2}\}$ and assume that there is a data signal present at the image subcarrier and that the channel responses at the k^{th} subcarrier and its image are uncorrelated [18]. It is also emphasized that in single-carrier systems, IQI causes distortion to the signal from its own complex conjugate while in multi-carrier systems, IQI causes distortion to the transmitted signal at subcarrier k from its image signal at subcarrier $-k$.

A. Joint TX/RX impaired by IQI

Here, we consider the general scenario where both the TX and RX suffer from IQI. The instantaneous SINR per symbol at the input of the RX can be approximated as [18]

$$\gamma \approx \frac{|\xi_{11}|^2 + |\xi_{22}|^2\frac{\gamma_{\text{id}}(-k)}{\gamma_{\text{id}}(k)}}{|\xi_{12}|^2 + |\xi_{21}|^2\frac{\gamma_{\text{id}}(-k)}{\gamma_{\text{id}}(k)} + \frac{\Lambda}{\gamma_{\text{id}}(k)}} \tag{25}$$

where

$$\gamma_{\text{id}}(-k) = \frac{E_s}{N_0}|h(-k)|^2. \tag{26}$$

Therefore, for the case of given $\gamma_{id}(-k)$ and with the aid of (25), the conditional SINR CDF can be expressed as

$$F_{\gamma_{\text{IQI}}}(x|y) = 1 - \exp\left(\frac{-x\left(|\xi_{21}|^2 y + \Lambda\right) - |\xi_{22}|^2 y}{\overline{\gamma}\left(|\xi_{11}|^2 - x|\xi_{12}|^2\right)}\right) \tag{27}$$

where $y = \gamma_{id}(-k)$. Based on this, the unconditional CDF is obtained by integrating (27) over the rayleigh PDF, yielding

$$F_{\gamma_{\mathrm{IQI}}}(x) = 1 - \frac{\exp\left(-\frac{x\Lambda}{\overline{\gamma}\left(|\xi_{11}|^2 - x|\xi_{12}|^2\right)}\right)}{1 + \frac{x|\xi_{21}|^2 - |\xi_{22}|^2}{\left(|\xi_{11}|^2 - x|\xi_{12}|^2\right)}}, \quad 0 \le x \le \frac{|\xi_{11}|^2}{|\xi_{12}|^2} \tag{28}$$

whereas the SINR PDF is obtained as

$$f_{\gamma_{\mathrm{IQI}}}(x) = \frac{\frac{|\xi_{11}|^2\Lambda}{\overline{\gamma}} + \frac{d\left(|\xi_{11}|^2 - x|\xi_{12}|^2\right)}{\frac{|\xi_{11}|^2}{C} + x\left(|\xi_{21}|^2 - |\xi_{12}|^2\right)}}{\left(|\xi_{11}|^2 - x|\xi_{12}|^2\right)\left(\frac{|\xi_{11}|^2}{C} + x\left(|\xi_{21}|^2 - |\xi_{12}|^2\right)\right)} \times \exp\left(\frac{-x\Lambda}{\overline{\gamma}\left(|\xi_{11}|^2 - x|\xi_{12}|^2\right)}\right), \tag{29}$$

which is valid for $0 \le x \le |\xi_{11}|^2/|\xi_{12}|^2$, while C and d are given by

$$C = \frac{|\xi_{11}|^2}{|\xi_{11}|^2 - |\xi_{22}|^2} \tag{30}$$

and

$$d = |\xi_{11}|^2|\xi_{21}|^2 - |\xi_{22}|^2|\xi_{12}|^2. \tag{31}$$

Proposition 2. *The MGF of multi-carrier systems impaired by joint TX/RX IQI is given by*

$$\mathcal{M}_{\gamma_{\mathrm{IQI}}}(s) = C + \frac{|\xi_{12}|^2 C}{s|\xi_{11}|^2}\exp\left(s\frac{|\xi_{11}|^2}{|\xi_{12}|^2} + \frac{\Lambda}{|\xi_{12}|^2\overline{\gamma}}\right) \times \gamma\left(2, s\frac{|\xi_{11}|^2}{|\xi_{12}|^2}; s\frac{|\xi_{11}|^2\Lambda}{|\xi_{12}|^4\overline{\gamma}}\right) \tag{32}$$

for $|\xi_{12}|^2 = |\xi_{21}|^2$,

$$\mathcal{M}_{\gamma_{\mathrm{IQI}}}(s) = C + \sum_{k=0}^{\infty}\frac{(-1)^k s^k d^k \exp\left(\frac{\Lambda}{|\xi_{12}|^2\overline{\gamma}} + s\frac{|\xi_{11}|^2}{|\xi_{12}|^2}\right)}{\left(|\xi_{12}|^2 - |\xi_{21}|^2\right)^{k+1}|\xi_{12}|^{2k-2}} \times \gamma\left(1-k, s\frac{|\xi_{11}|^2}{|\xi_{12}|^2}; s\frac{|\xi_{11}|^2\Lambda}{|\xi_{12}|^4\overline{\gamma}}\right) \tag{33}$$

for $\left|\frac{|\xi_{11}|^2|\xi_{21}|^2 - |\xi_{22}|^2|\xi_{12}|^2}{|\xi_{12}|^2 - |\xi_{21}|^2}\right| < |\xi_{11}|^2$, *and*

$$\mathcal{M}_{\gamma_{\mathrm{IQI}}}(s) = C + \exp\left(s\frac{|\xi_{11}|^2}{|\xi_{12}|^2} + \frac{\Lambda}{|\xi_{12}|^2\overline{\gamma}}\right)\sum_{k=0}^{\infty}\frac{|\xi_{12}|^{2k+4}}{d^{k+1}s^{k+1}} \times \left(|\xi_{21}|^2 - |\xi_{12}|^2\right)^k \gamma\left(k+2, s\frac{|\xi_{11}|^2}{|\xi_{12}|^2}; s\frac{|\xi_{11}|^2\Lambda}{|\xi_{12}|^4\overline{\gamma}}\right) \tag{34}$$

for $\left|\frac{|\xi_{11}|^2|\xi_{21}|^2 - |\xi_{22}|^2|\xi_{12}|^2}{|\xi_{12}|^2 - |\xi_{21}|^2}\right| > |\xi_{11}|^2$, *where* $\gamma(\alpha, x; b) = \int_0^x t^{\alpha-1}\exp\left(-t - \frac{b}{t}\right)\mathrm{d}t$ *is the extended lower incomplete Gamma function [43].*

Proof. The proof is provided in Appendix B. □

B. TX Impaired by IQI

Assuming that the RX RF front-end is ideal, while the TX experiences IQI, the instantaneous SINR per symbol at the input of the RX is given by

$$\gamma_{\mathrm{IQI}} = \frac{|\mu_t|^2}{|\nu_t|^2 + \frac{1}{\gamma_{\mathrm{id}}(k)}}. \tag{35}$$

Hence, by setting $\mu_r = 1$ and $\nu_r = 0$ in (28), it follows that

$$F_{\gamma_{\mathrm{IQI}}}(x) = 1 - \exp\left(-\frac{1}{\overline{\gamma}\left(\frac{|\mu_t|^2}{x} - |\nu_t|^2\right)}\right), \quad 0 \le x \le \frac{|\mu_t|^2}{|\nu_t|^2} \tag{36}$$

which yields straightforwardly the corresponding SINR PDF, namely

$$f_{\gamma_{\mathrm{IQI}}}(x) = \frac{|\mu_t|^2\exp\left(-\frac{1}{\overline{\gamma}\left(\frac{|\mu_t|^2}{x} - |\nu_t|^2\right)}\right)}{\overline{\gamma}\left(|\mu_t|^2 - x|\nu_t|^2\right)^2} \tag{37}$$

which is valid for $0 \le x \le |\mu_t|^2/|\nu_t|^2$. It is noted that (37) is similar to (23) for $\alpha = |\mu_t|^2$, $\beta = |\nu_t|^2$, and $A = 1$. Hence, with the aid of (24), the instantaneous SINR MGF of multi-carrier systems experiencing TX IQI only is given by

$$\mathcal{M}_{\gamma_{\mathrm{IQI}}}(s) = \exp\left(\frac{|\mu_t|^2}{|\nu_t|^2}s + \frac{1}{|\nu_t|^2\overline{\gamma}}\right)\Gamma\left(1, \frac{1}{\overline{\gamma}|\nu_t|^2}; \frac{s|\mu_t|^2}{|\nu_t|^4\overline{\gamma}}\right), \tag{38}$$

which is also novel.

C. RX Impaired by IQI

Assuming that the TX RF front-end is ideal, while the RX is impaired by IQI, the instantaneous SINR per symbol at the input of the RX is expressed as

$$\gamma_{\mathrm{IQI}} = \frac{|\mu_r|^2}{|\nu_r|^2\frac{\gamma_{\mathrm{id}}(-k)}{\gamma_{\mathrm{id}}(k)} + \frac{\Lambda}{\gamma_{\mathrm{id}}(k)}}. \tag{39}$$

Hence, substituting $\mu_t = 1$ and $\nu_t = 0$ in (28) one obtains

$$F_{\gamma_{\mathrm{IQI}}}(x) = 1 - \frac{|\mu_r|^2}{|\mu_r|^2 + x|\nu_r|^2}\exp\left(-\frac{x}{\overline{\gamma}}\left(1 + \frac{|\nu_r|^2}{|\mu_r|^2}\right)\right), \tag{40}$$

which is valid for $0 \le x \le \infty$. With the aid of (29) and after some algebraic manipulations, the respective SINR PDF is deduced

$$f_{\gamma_{\mathrm{IQI}}}(x) = \frac{1 + \frac{|\nu_r|^2}{|\mu_r|^2} + \frac{\overline{\gamma}|\nu_r|^2}{|\mu_r|^2\left(\frac{x|\nu_r|^2}{|\mu_r|^2} + 1\right)}}{\overline{\gamma}\left(\frac{x|\nu_r|^2}{|\mu_r|^2} + 1\right)}\exp\left(-\frac{x\left(\frac{|\nu_r|^2}{|\mu_r|^2} + 1\right)}{\overline{\gamma}}\right) \tag{41}$$

which is valid for $0 \le x \le \infty$.

Finally, from (56) and (41), the corresponding MGF is obtained as

$$\mathcal{M}_{\gamma_{\mathrm{IQI}}}(s) = \frac{1 + \frac{|\mu_r|^2}{|\nu_r|^2}}{\overline{\gamma}}\int_0^{\infty}\frac{\exp\left(-x\left(\frac{1}{\overline{\gamma}} + \frac{|\nu_r|^2}{\overline{\gamma}|\mu_r|^2} - s\right)\right)}{x + \frac{|\mu_r|^2}{|\nu_r|^2}}dx + \int_0^{\infty}\frac{\exp\left(-x\left(\frac{1}{\overline{\gamma}} + \frac{|\nu_r|^2}{\overline{\gamma}|\mu_r|^2} - s\right)\right)}{\left(x + \frac{|\mu_r|^2}{|\nu_r|^2}\right)^2}\mathrm{d}x \tag{42}$$

which with the aid of [44, eq. (3.352)] and [44, eq. (3.353)], eq. (42) can be expressed by the following closed-form representation

$$\mathcal{M}_{\gamma_{\mathrm{IQI}}}(s) = 1 - s\frac{|\mu_r|^2}{|\nu_r|^2}\exp\left(\frac{1}{\overline{\gamma}} + \frac{|\mu_r|^2}{\overline{\gamma}|\nu_r|^2} - \frac{s|\mu_r|^2}{|\nu_r|^2}\right) \times \mathrm{Ei}\left(-\frac{1}{\overline{\gamma}} - \frac{|\mu_r|^2}{\overline{\gamma}|\nu_r|^2} + \frac{s|\mu_r|^2}{|\nu_r|^2}\right) \tag{43}$$

where $\mathrm{Ei}(z) = -\int_{-z}^{\infty}\exp(-t)/t\mathrm{d}t$ denotes the exponential integral function [44].

The different MGF expressions derived are summarized in Table II. It is noted that with the aid of the derived MGFs, the SER of various M-ary modulation schemes under different IQI effects as well as multi-channel reception schemes can be readily determined.

V. Symbol Error Rate Analysis

This section capitalizes on the derived MGF representation and evaluates the SER performance of both single-carrier and multi-carrier systems employing different coherent and noncoherent *M*-ary modulation schemes in the presence of IQI and multipath fading.

A. Coherent M-PSK Symbol Error Rate Analysis

For coherently detected *M*-PSK, the SER under AWGN is given by [38, eq. (8.22)]. Under fading conditions, the average SER is obtained by averaging [38, eq. (8.22)] over the considered channel's SNR PDF, namely

$$P_{s,\mathrm{PSK}} = \frac{1}{\pi}\int_0^{\tilde{M}} \mathcal{M}_{\gamma_{\mathrm{IQI}}}\left(-\frac{g}{\sin^2(\theta)}\right)\mathrm{d}\theta. \tag{44}$$

where $\tilde{M} = (M-1)/M$ and $g = \sin^2\left(\frac{\pi}{M}\right)$. Therefore, assuming PSK modulation under IQI, the average SER of the different impairment scenarios considered for both single-carrier and multi-carrier systems, can be obtained by substituting the derived MGFs from Table II in (44), which for single-carrier systems is given by

$$P_{s,\mathrm{PSK}} = \frac{1}{\pi}\int_0^{\tilde{M}} \exp\left(-\frac{g\alpha}{\sin^2(\theta)\beta} + \frac{A}{\beta\overline{\gamma}}\right) \times \Gamma\left(1, \frac{A}{\overline{\gamma}\beta}; -\frac{g\alpha A}{\sin^2(\theta)\beta^2\overline{\gamma}}\right)\mathrm{d}\theta \tag{45}$$

B. Coherent M-QAM Symbol Error Rate Analysis

For *M*-QAM modulation, the SER under AWGN is given by [38, eq. (8.13)]. Under fading conditions and IQI, the average SER is obtained as

$$P_{s,\mathrm{QAM}} = \frac{4}{\pi}\underline{M}\int_0^{\frac{\pi}{2}} \mathcal{M}_{\gamma_{\mathrm{IQI}}}\left(\frac{3}{2(M-1)\sin^2\theta}\right)\mathrm{d}\theta - \frac{4}{\pi}\underline{M}^2\int_0^{\frac{\pi}{4}} \mathcal{M}_{\gamma_{\mathrm{IQI}}}\left(\frac{3}{2(M-1)\sin^2\theta}\right)\mathrm{d}\theta. \tag{46}$$

where $\underline{M} = \left(\sqrt{M}-1\right)/\sqrt{M}$, and the average SER of the different impairment scenarios considered for both single-carrier and multi-carrier systems, can be obtained by substituting the derived MGFs from Table II into (46), which for single-carrier systems reduces to

$$P_{s,\mathrm{QAM}} = \frac{4}{\pi}\underline{M}\int_0^{\frac{\pi}{2}} \exp\left(\frac{3\alpha}{2\beta(M-1)\sin^2\theta} + \frac{A}{\beta\overline{\gamma}}\right) \times \Gamma\left(1, \frac{A}{\overline{\gamma}\beta}; \frac{3\alpha A}{\beta^2\overline{\gamma}2(M-1)\sin^2\theta}\right)\mathrm{d}\theta - \frac{4}{\pi}\underline{M}^2\int_0^{\frac{\pi}{4}} \exp\left(\frac{3\alpha}{2\beta(M-1)\sin^2\theta} + \frac{A}{\beta\overline{\gamma}}\right) \times \Gamma\left(1, \frac{A}{\overline{\gamma}\beta}; \frac{3\alpha A}{\beta^2\overline{\gamma}2(M-1)\sin^2\theta}\right)\mathrm{d}\theta. \tag{47}$$

C. Differential M-PSK Symbol Error Rate Analysis

Considering differential detection of *M*-PSK over fading channels, the SER is given by [38, eq. (8.166)]. Hence, the average symbol error rate for *M*-DPSK over Rayleigh fading channels for both single-carrier and multi-carrier systems, in the presence of IQI can be obtained by substituting the derived MGFs from Table II, which for multi-carrier systems with TX IQI only is given by

$$P_{s,\mathrm{DPSK}} = \frac{1}{\pi}\int_0^{\tilde{M}} \exp\left(-\frac{|\mu_t|^2 g}{|\nu_t|^2(1+\rho\cos(\theta))} + \frac{1}{|\nu_t|^2\overline{\gamma}}\right) \times \Gamma\left(1, \frac{1}{\overline{\gamma}|\nu_t|^2}, \frac{-g|\mu_t|^2}{(1+\rho\cos(\theta))|\nu_t|^4\overline{\gamma}}, 1\right)\mathrm{d}\theta \tag{48}$$

where $\rho = \sqrt{1-g}$.

D. Noncoherent M-FSK Symbol Error Rate Analysis

Assuming noncoherent detection of orthogonal signals, corresponding to a minimum frequency spacing $\Delta f = 1/T_s$, the SER of *M*-FSK over fading channels is given by [38, eq. (8.158)]. Therefore, substituting the derived MGF expressions from Table II in [38, eq. (8.158)] yields the average SER of single-carrier and multi-carrier systems in the presence of IQI, which for the case of multi-carrier systems with RX IQI only is given by

$$P_{s,\mathrm{FSK}} = \sum_{k=1}^{M-1}\frac{(-1)^{k+1}}{k+1}\binom{M-1}{k} \times \left[1 + \frac{k|\mu_r|^2\mathrm{Ei}\left(-\frac{\Lambda}{\overline{\gamma}|\nu_r|^2} - \frac{k|\mu_r|^2}{(k+1)|\nu_r|^2}\right)}{\exp\left(-\frac{\Lambda}{\overline{\gamma}|\nu_r|^2} - \frac{k|\mu_r|^2}{(k+1)|\nu_r|^2}\right)(k+1)|\nu_r|^2}\right]. \tag{49}$$

To the best of the authors' knowledge, the derived analytic expressions have not been previously reported in the open technical literature.

TABLE II: SINR MGFs

	Single-carrier systems	Multi-carrier systems
TX IQI	$\mathcal{M}_{\gamma_{\mathrm{IQI}}}(s)=\exp\left(\frac{\lvert\mu_t\rvert^2}{\lvert\nu_t\rvert^2}s+\frac{1}{\lvert\nu_t\rvert^2\overline{\gamma}}\right)\Gamma\left(1,\frac{1}{\overline{\gamma}\lvert\nu_t\rvert^2};\frac{s\lvert\mu_t\rvert^2}{\lvert\nu_t\rvert^4\overline{\gamma}}\right)$	
RX IQI	$\mathcal{M}_{\gamma_{\mathrm{IQI}}}(s)=\exp\left(\frac{\lvert\mu_r\rvert^2 s}{\lvert\nu_r\rvert^2}+\frac{\Lambda}{\lvert\nu_r\rvert^2\overline{\gamma}}\right)\Gamma\left(1,\frac{\Lambda}{\overline{\gamma}\lvert\nu_r\rvert^2};\frac{s\lvert\mu_r\rvert^2\Lambda}{\lvert\nu_r\rvert^4\overline{\gamma}}\right)$	$\mathcal{M}_{\gamma_{\mathrm{IQI}}}(s)= 1-s\frac{\lvert\mu_r\rvert^2}{\lvert\nu_r\rvert^2}\exp\left(\frac{1}{\overline{\gamma}}+\frac{\lvert\mu_r\rvert^2}{\overline{\gamma}\lvert\nu_r\rvert^2}-\frac{s\lvert\mu_r\rvert^2}{\lvert\nu_r\rvert^2}\right)\times\mathrm{Ei}\left(-\frac{1}{\overline{\gamma}}-\frac{\lvert\mu_r\rvert^2}{\overline{\gamma}\lvert\nu_r\rvert^2}+\frac{s\lvert\mu_r\rvert^2}{\lvert\nu_r\rvert^2}\right)$
Joint IQI	$\mathcal{M}_{\gamma_{\mathrm{IQI}}}(s)= \exp\left(\frac{\lvert\xi_{11}\rvert^2+\lvert\xi_{22}\rvert^2}{\lvert\xi_{12}\rvert^2+\lvert\xi_{21}\rvert^2}s+\frac{\Lambda}{(\lvert\xi_{12}\rvert^2+\lvert\xi_{21}\rvert^2)\overline{\gamma}}\right)\times\Gamma\left(1,\frac{\Lambda}{\overline{\gamma}(\lvert\xi_{12}\rvert^2+\lvert\xi_{21}\rvert^2)};\frac{s(\lvert\xi_{11}\rvert^2+\lvert\xi_{22}\rvert^2)\Lambda}{(\lvert\xi_{12}\rvert^2+\lvert\xi_{21}\rvert^2)^2\overline{\gamma}}\right)$	$\mathcal{M}_{\gamma_{\mathrm{IQI}}}(s)= C+\frac{\lvert\xi_{12}\rvert^2}{s(\lvert\xi_{11}\rvert^2-\lvert\xi_{22}\rvert^2)}\exp\left(s\frac{\lvert\xi_{11}\rvert^2}{\lvert\xi_{12}\rvert^2}+\frac{\Lambda}{\lvert\xi_{12}\rvert^2\overline{\gamma}}\right)\times\gamma\left(2,s\frac{\lvert\xi_{11}\rvert^2}{\lvert\xi_{12}\rvert^2};s\frac{\lvert\xi_{11}\rvert^2\Lambda}{\lvert\xi_{12}\rvert^4\overline{\gamma}}\right),$ for $\lvert\xi_{12}\rvert^2=\lvert\xi_{21}\rvert^2$
		$\mathcal{M}_{\gamma_{\mathrm{IQI}}}(s)= C+\sum_{k=0}^{\infty}\frac{(-s)^k d^k\exp\left(s\frac{\lvert\xi_{11}\rvert^2}{\lvert\xi_{12}\rvert^2}\right)}{(\lvert\xi_{12}\rvert^2-\lvert\xi_{21}\rvert^2)^{k+1}\lvert\xi_{12}\rvert^{2k-2}}\times\exp\left(\frac{\Lambda}{\lvert\xi_{12}\rvert^2\overline{\gamma}}\right)\gamma\left(1-k,s\frac{\lvert\xi_{11}\rvert^2}{\lvert\xi_{12}\rvert^2};s\frac{\lvert\xi_{11}\rvert^2\Lambda}{\lvert\xi_{12}\rvert^4\overline{\gamma}}\right),$ for $\left\lvert\frac{\lvert\xi_{11}\rvert^2\lvert\xi_{21}\rvert^2-\lvert\xi_{22}\rvert^2\lvert\xi_{12}\rvert^2}{\lvert\xi_{12}\rvert^2-\lvert\xi_{21}\rvert^2}\right\rvert<\lvert\xi_{11}\rvert^2$
		$\mathcal{M}_{\gamma_{\mathrm{IQI}}}(s)= C+\sum_{k=0}^{\infty}\frac{\lvert\xi_{12}\rvert^{2k+4}\exp\left(s\frac{\lvert\xi_{11}\rvert^2}{\lvert\xi_{12}\rvert^2}\right)}{(\lvert\xi_{21}\rvert^2-\lvert\xi_{12}\rvert^2)^{-k}d^{k+1}s^{k+1}}\times\exp\left(\frac{\Lambda}{\lvert\xi_{12}\rvert^2\overline{\gamma}}\right)\gamma\left(k+2,s\frac{\lvert\xi_{11}\rvert^2}{\lvert\xi_{12}\rvert^2};s\frac{\lvert\xi_{11}\rvert^2\Lambda}{\lvert\xi_{12}\rvert^4\overline{\gamma}}\right),$ for $\left\lvert\frac{\lvert\xi_{11}\rvert^2\lvert\xi_{21}\rvert^2-\lvert\xi_{22}\rvert^2\lvert\xi_{12}\rvert^2}{\lvert\xi_{12}\rvert^2-\lvert\xi_{21}\rvert^2}\right\rvert>\lvert\xi_{11}\rvert^2$

VI. Extension to MIMO Systems

In this section, we provide deep insights into the performance of multichannel receivers. To this end, we consider the case of independent but not identically distributed ($i.n.i.d.$) L-branch MRC diversity receiver for coherently detected M-PSK and M-QAM modulations and the case of differential STBC.

A. Maximum Ratio Combining

The MRC scheme is the optimal combining scheme at the expense of increased complexity, where the receiver requires knowledge of all channel fading parameters [38], [45]. Here, the receiver coherently combines all received signals, resulting in the following MGF

$$\begin{aligned}\mathcal{M}_{\gamma_{MRC}}(s)&=\mathbb{E}\left[e^{-s\sum_{k=1}^{L}\gamma_k}\right]\\&=\prod_{k=1}^{L}\mathcal{M}_{\gamma_k}(s),\end{aligned}\tag{50}$$

where γ_k is the instantaneous SNR of the k^{th} branch.

B. Differential STBC

Here, we consider the differential Alamouti Space-Time Block Codes (STBC)-OFDM system with two transmit antenna and a single receive antenna. Assuming that both the TX and RX are impaired by IQI, the instantaneous SINR at the k^{th} subcarrier is given by [37], [46]

$$\gamma_{\mathrm{IQI}}(k)\approx\frac{(1-\epsilon_{TX})\left(\gamma_{\mathrm{id}_1}(k)+\gamma_{\mathrm{id}_2}(k)\right)}{4\left(1+\frac{\lvert\mu_r\rvert^2}{\lvert\nu_r\rvert^2\overline{\gamma}}\right)}\tag{51}$$

where $\gamma_{\mathrm{id}_i}(k)$ is the ideal instantaneous SNR of subcarrier k at the i^{th} antenna and

$$\epsilon_{TX}=2.5\left(1+\cot\left(\frac{\pi}{M}\right)^2\right)\frac{\lvert\mu_t\rvert^2}{\lvert\nu_t\rvert^2}.\tag{52}$$

From (51), the corresponding SINR MGF is obtained as

$$\mathcal{M}_{\gamma_{\mathrm{IQI}}}(s)=\mathcal{M}_{\gamma_{id,1}}\left(s\overline{\Gamma}\right)\mathcal{M}_{\gamma_{\mathrm{id},2}}\left(s\overline{\Gamma}\right)\tag{53}$$

where

$$\overline{\Gamma}=\frac{4\left(1+\frac{\lvert\mu_r\rvert^2}{\lvert\nu_r\rvert^2\overline{\gamma}}\right)}{(1-\epsilon_{TX})}\tag{54}$$

and $\mathcal{M}_{\gamma_{id,j}}$, $j\epsilon\{1,2\}$ is the MGF of the IQI free SNR given by [38]

$$\mathcal{M}_{\gamma_{id,j}}=\frac{1}{1-s\overline{\Gamma}}\tag{55}$$

Hence, the corresponding SER is obtained by substituting (53) in the general SER expression for PSK signals in (44). It is noted that the analysis can be easily extended to more than two antenna scenario [37]. Moreover, the cases of TX IQI only and RX IQI only can be obtained by setting $\lvert\mu_r\rvert^2=1,\lvert\nu_r\rvert^2=0$ and $\lvert\mu_t\rvert^2=1,\lvert\nu_t\rvert^2=0$, respectively.

VII. Numerical and Simulation Results

In this section, we quantify the effects of IQI on the performance of single-carrier and multi-carrier based *M*-PSK, *M*-DPSK, *M*-QAM and *M*-FSK systems over Rayleigh fading channels in terms of the corresponding average SER. It is noted that, for a fair comparison, we assume that the transmit power level is always fixed. This implies that the transmitted signal is normalized by $\lvert\mu_t\rvert^2+\lvert\nu_t\rvert^2$ for TX IQI, by $\lvert\mu_r\rvert^2+\lvert\nu_r\rvert^2$ for RX IQI and by $\left(\lvert\mu_t\rvert^2+\lvert\nu_t\rvert^2\right)\left(\lvert\mu_r\rvert^2+\lvert\nu_r\rvert^2\right)$ for joint

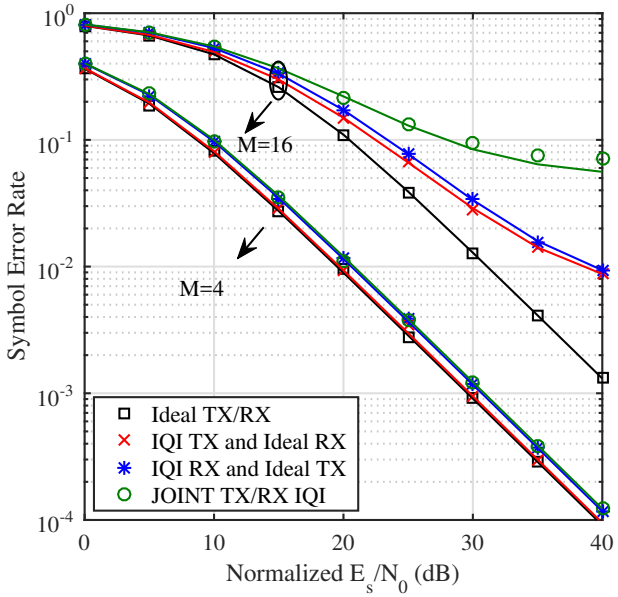

Fig. 1: Single-carrier system average SER as a function of the normalized E_s/N_0 for M-PSK when $\mathrm{IRR}_t = \mathrm{IRR}_r = 20\mathrm{dB}$ and $\phi = 3°$.

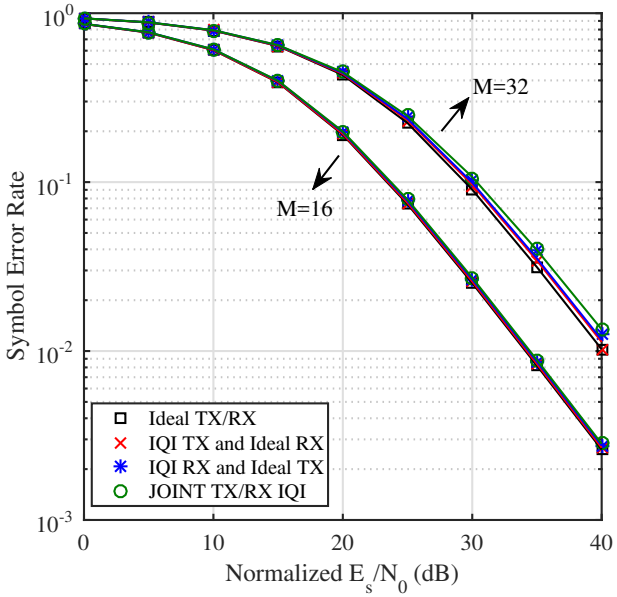

Fig. 3: Single-carrier system average SER as a function of the normalized E_s/N_0 for M-DPSK when $\mathrm{IRR}_t = \mathrm{IRR}_r = 35\mathrm{dB}$ and $\phi = 1°$.

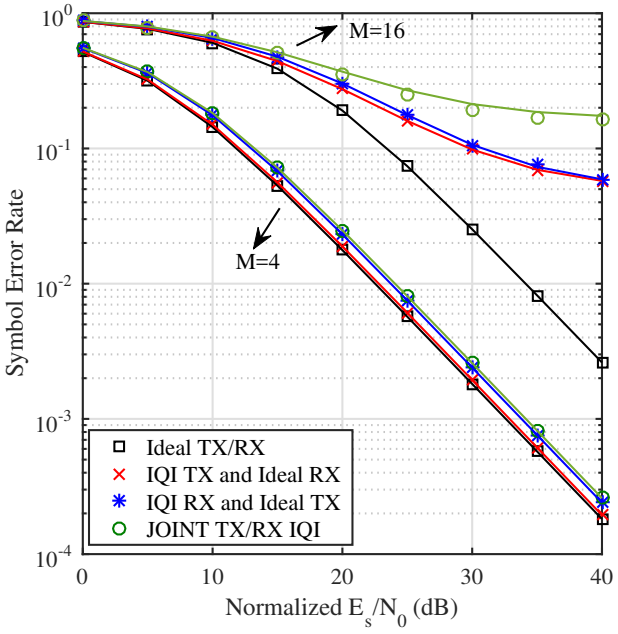

Fig. 2: Single-carrier system average SER as a function of the normalized E_s/N_0 for M-DPSK when $\mathrm{IRR}_t = \mathrm{IRR}_r = 20\mathrm{dB}$ and $\phi = 3°$.

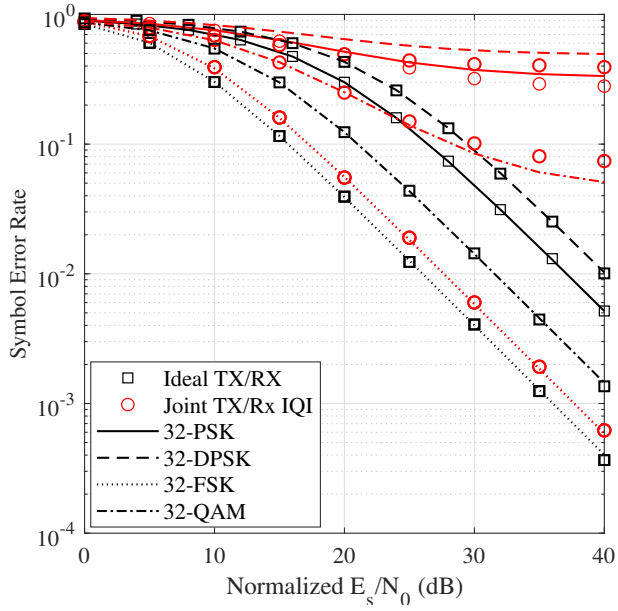

Fig. 4: Single-carrier system average SER as a function of the normalized E_s/N_0 for 32-PSK, 32-DPSK, 32-FSK and 32-QAM when $\mathrm{IRR}_t = \mathrm{IRR}_r = 20\mathrm{dB}$ and $\phi = 3°$.

TX/RX IQI. To this end, Figs. 1−5 and Figs. 6−12 illustrate the SER for single-carrier systems and multi-carrier systems, respectively. It is noted that the numerical results are shown with lines, whereas markers are used to illustrate the respective computer simulation results. For both single-carrier and multi-carrier systems, it is noticed that the derived expressions perfectly match the simulation results for the cases of TX and RX IQI; while for the case of joint TX/RX IQI, the approximation adopted in (19) and (25) and the assumption of uncorrelated subcarriers do not significantly affect the accuracy of the SER analysis.

A. *Single-Carrier Systems*

Assuming single-carrier transmission over flat Rayleigh fading channels, it is first observed that overall, RX IQI has

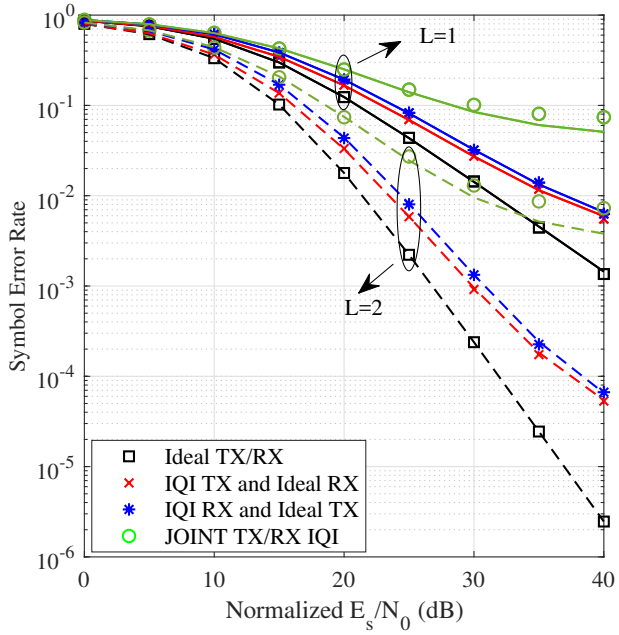

Fig. 5: Single-carrier system average SER as a function of the normalized E_s/N_0 for L-branch 32-QAM MRC receiver when $\text{IRR}_t = \text{IRR}_r = 20\text{dB}$ and $\phi = 3°$.

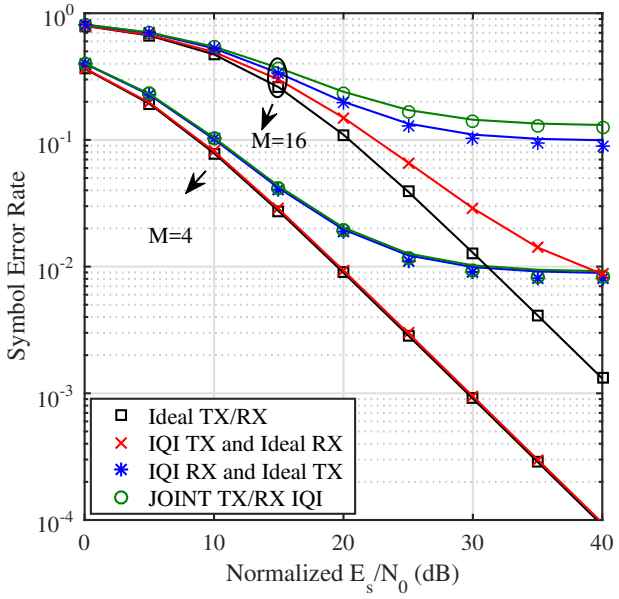

Fig. 6: Multi-carrier system average SER as a function of the normalized E_s/N_0 for M-PSK when $\text{IRR}_t = \text{IRR}_r = 20\text{dB}$ and $\phi = 3°$.

more detrimental impact on the system performance than TX IQI. This result is expected since RX IQI affects both the signal and the noise while TX IQI impairs the information signal only. However, when the modulation order is increased, as shown in Figs. 1-2 TX IQI causes performance degradation that is quite comparable to RX IQI.

It is also noticed that IQI exhibits different levels of degradation on the performance of the different modulation schemes considered. For example, it is shown in Fig. 4 that joint TX/RX IQI only slightly affects the performance of 32-FSK. On the other hand, it is shown that IQI causes an error floor for the other three candidate modulation schemes. As shown in Fig. 5, this error floor is manifested in both single-antenna and multi-antenna receivers. This can be explained by the fact that the tone spacing in FSK is constant regardless of the modulation order. Hence, unlike PSK, DPSK and QAM modulations, the IQI effects on FSK do not depend on the modulation order. However, the cost of increasing M for FSK is an increased transmission bandwidth. This is not the case for the other three modulation schemes where the distance between constellation points is hughly affected by the modulation order. For instance, the effects of IQI can be considered acceptable i.e., no error floor observed for the considered SNR range, only for $M = 4$ for PSK and DPSK based systems. In fact, for single-carrier systems, when $M = 16$, an error floor is observed at around 35dB when PSK modulation suffers from joint TX/RX IQI, while for DPSK this error floor appears at around 30dB for all the considered impairment scenarios. It is also worth mentioning that for the joint TX/RX IQI case, this error floor is around 6×10^{-2} for PSK versus 2×10^{-1} for DPSK. Moreover, depending on the considered system's parameters, the level of performance degradation caused by this impairment can differ significantly. In particular, it is observed that, in some cases, compensating IQI will only result in added complexity since the effects of the impairment are negligible. This is the case for single-carrier systems with high TX/RX IRR, presented in Fig. 3, and single-carrier FSK for all the practical levels of IRR.

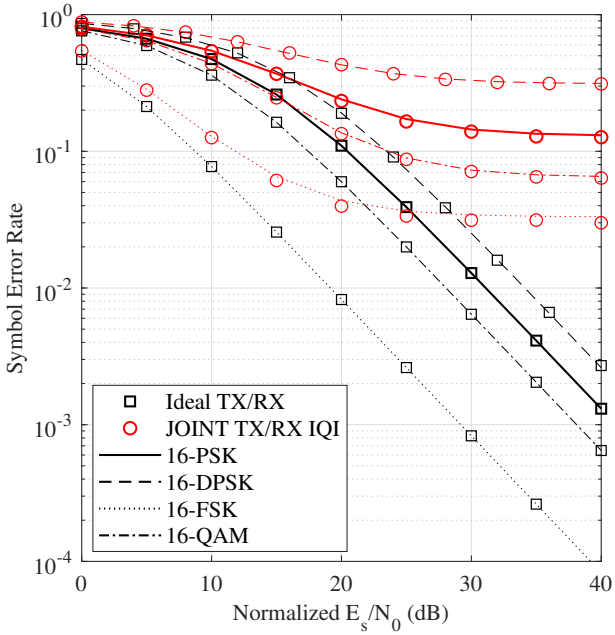

Fig. 7: Multi-carrier system average SER as a function of the normalized E_s/N_0 for 16-PSK, 16-DPSK, 16-FSK and 16-QAM when $\text{IRR}_t = \text{IRR}_r = 20\text{dB}$ and $\phi = 3°$.

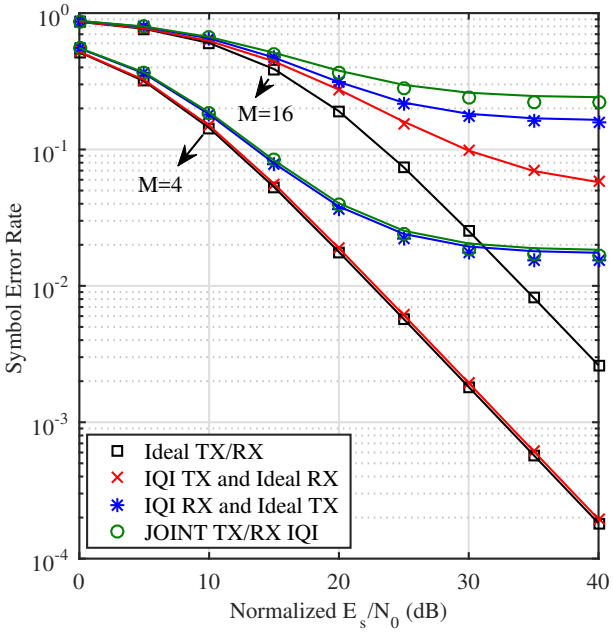

Fig. 8: Multi-carrier system average SER as a function of the normalized E_s/N_0 for M-DPSK when $\mathrm{IRR}_t = \mathrm{IRR}_r = 20\mathrm{dB}$ and $\phi = 3°$.

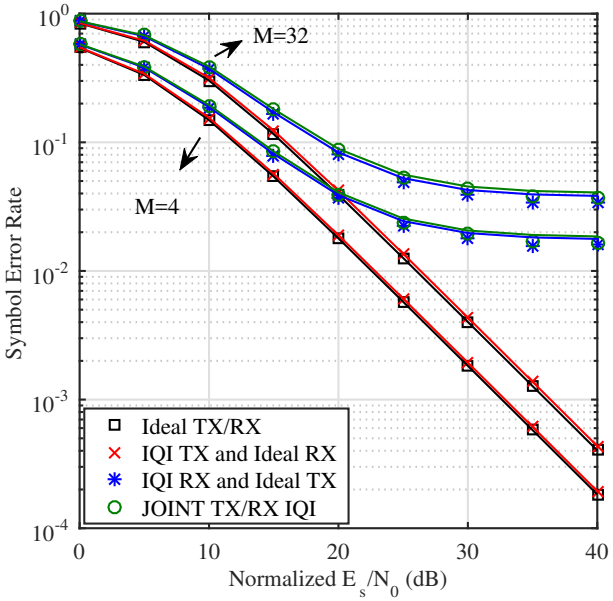

Fig. 9: Multi-carrier system average SER as a function of the normalized E_s/N_0 for M-FSK when $\mathrm{IRR}_t = \mathrm{IRR}_r = 20\mathrm{dB}$ and $\phi = 3°$.

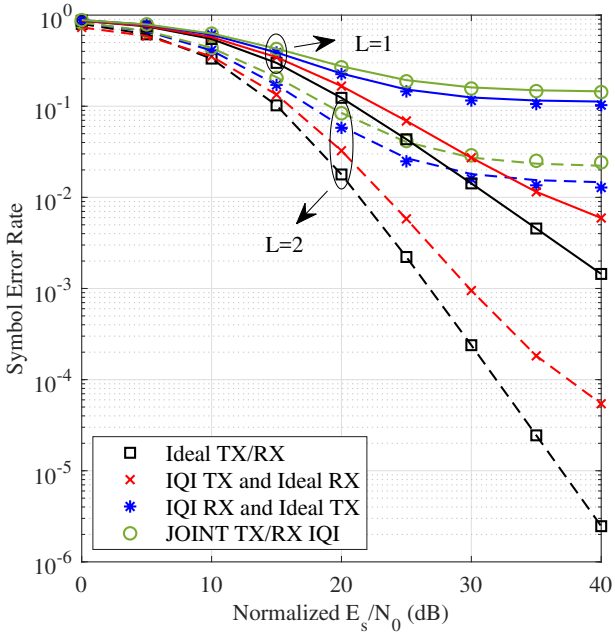

Fig. 10: Multi-carrier system average SER as a function of the normalized E_s/N_0 for L-branch 32-QAM MRC receiver when $\mathrm{IRR}_t = \mathrm{IRR}_r = 20\mathrm{dB}$ and $\phi = 3°$.

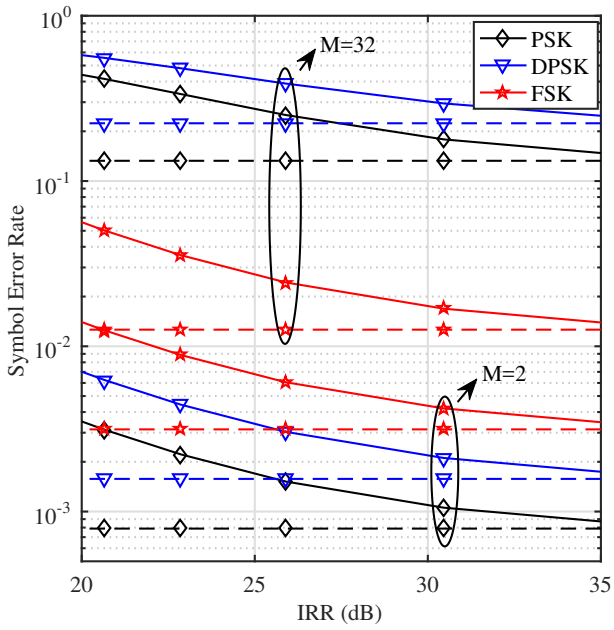

Fig. 11: Multi-carrier system average SER as a function of the IRR for M-PSK, M-DPSK and M-FSK, with RX IQI only, when $E_s/N_0 = 25\mathrm{dB}$ and $\phi = 2°$.

B. Multi-Carrier Systems

Here, we assume a multipath channel with 8 independent and identically distributed taps where each tap is a zero-mean complex Gaussian random variable [47]. Even though the effects of IQI on the different modulation schemes follow the same trend in multi-carrier systems as in single-carrier systems, it is observed that IQI affects the former more severely than the latter. This is because IQI in multi-carrier systems causes interference from the image subcarrier, which could benefit from better fading conditions than the desired signal. An interesting example is the case of M-FSK constellation,

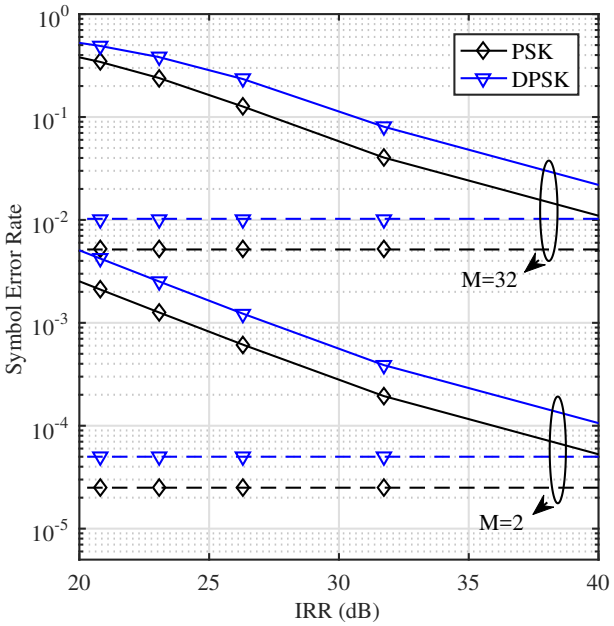

Fig. 12: Multi-carrier system average SER as a function of the IRR for *M*-PSK and *M*-DPSK, with RX IQI only, when $E_s/N_0 = 40\text{dB}$ and $\phi = 1°$.

where an error floor is observed in Fig. 9, regardless of the modulation order, for the cases of RX IQI only and joint TX/RX IQI cases. In the same context, the error floor for 4-PSK appears at around 25dB. This error floor is observed for FSK and DPSK as well. Moreover, we notice that 4-FSK is the most robust towards IQI among the considered modulations, since the error floor appears at around 30dB.

It is also noted that for $\text{IRR}_t = \text{IRR}_r = 20\text{dB}$, in multi-carrier systems, the effects of IQI at the RX should be compensated in order to achieve a reliable communication link, even in the case of the relatively simple binary modulation schemes and multi-antenna receivers. For these scenarios the amount of performance degradation observed depends on the modulation order, the SNR, the impairment scenario and the IQI level. Hence, in particular cases, such as in low modulation orders of PSK and DPSK modulations, as well as M-FSK, compensation can be implemented at the RX front-end only in order to achieve a reliable performance. On the contrary, in other cases compensation of both TX/RX IQI is required in order to achieve a reliable communication link.

Finally, Fig. 11 and Fig. 12 demonstrate the effects of the IRR on the SER of the different considered modulation schemes, when $\text{SNR} = 25\text{dB}$ and $\text{SNR} = 40\text{dB}$, respectively. It is assumed that both TX and RX are IQI-impaired and that $\text{IRR}_t = \text{IRR}_r$. The phase imbalance assumed is 1° in Fig. 11 and 2° in Fig. 12. It is also noted that the continuous lines and dashed lines correspond to the IQI-impaired and ideal cases, respectively. For moderate SNR values, one can see that IQI affects the different modulations schemes in a different manner. For instance, joint TX/ RX IQI exhibits a constant loss in the SER performance of M-FSK regardless of the modulation order, which is not the case when considering phase modulation. Moreover, it is noticed that for lower SNR values, the effects of IQI vanish when the IRR is increased; while, for higher SNR values and given that IQI effects dominate noise effects at high SNR, there is a noticeable performance degradation even when considering high IRR values.

VIII. Conclusion

We developed a general framework for the SER performance analysis of different *M*-ary coherent and noncoherent modulation schemes over Rayleigh fading channels in the presence of IQI at the RF front end. The realistic cases of TX IQI only, RX IQI only and joint TX/RX IQI were considered and the corresponding average SER expression of the underlying schemes was derived both in exact and in asymptotic form providing useful insights into the overall system behavior. The derived analytic results were corroborated with respective results from computer simulations. It was shown that the performance degradation caused by IQI greatly depends on the considered communication system's parameters including the modulation scheme. Moreover, for coherent and noncoherent phase modulation, increasing the modulation order increases the impact of IQI on the system. As for the case of frequency modulation the performance degradation observed is constant regardless of the modulation order and single-carrier frequency modulation is the most robust scheme to IQI effects. Additionally, it was shown that the effects of this impairments can be quite significant on the SER performance of the system; hence, the optimal compensation strategy to adopt greatly depends on the system's parameters. This highlights the importance of accurate characterization of this impairment in order to achieve a reliable communication link with minimal added complexity.

Appendix A
Derivation of MGF for Single-Carrier Systems Impaired by IQI

By recalling that [38]

$$\mathcal{M}_{\gamma_{\text{IQI}}}(s) = \int_0^\infty \exp(sx)\, f_{\gamma_{\text{IQI}}}(x)\, \mathrm{d}x \tag{56}$$

and substituting (23) into (56) yields

$$\mathcal{M}_{\gamma_{\text{IQI}}}(s) = \int_0^{\frac{\alpha}{\beta}} \exp(sx)\, \frac{\alpha A \exp\left(-\frac{A}{\overline{\gamma}\left(\frac{\alpha}{x}-\beta\right)}\right)}{\overline{\gamma}\,(\alpha - x\beta)^2}\mathrm{d}x. \tag{57}$$

By also considering the change of variable $y = \alpha - \gamma\beta$ and after some mathematical manipulations, one obtains

$$\mathcal{M}_{\gamma_{\text{IQI}}}(s) = \frac{\alpha A \exp\left(\frac{\alpha\overline{\gamma}s + A}{\beta\overline{\gamma}}\right)}{\overline{\gamma}\beta} \int_0^\alpha \exp\left(-\frac{sy}{\beta} - \frac{\alpha A}{\beta\overline{\gamma}y}\right)\mathrm{d}y. \tag{58}$$

Based on this and by taking $z = \frac{\alpha A}{\beta\overline{\gamma}y}$, equation (24) is deduced, which completes the proof.

APPENDIX B
DERIVATION OF MGF FOR MULTI-CARRIER SYSTEMS IMPAIRED BY JOINT TX/RX IQI

From (56) and (29), taking $u = \exp(s\gamma)$ and $dv = f_\gamma(\gamma)$ and integrating by parts, one obtains

$$\mathcal{M}_{\gamma_{\mathrm{IQI}}}(s) = C + s\int_0^{\frac{|\xi_{11}|^2}{|\xi_{12}|^2}} \frac{|\xi_{11}|^2 - x|\xi_{12}|^2}{\frac{|\xi_{11}|^2}{C} + x\left(|\xi_{21}|^2 - |\xi_{12}|^2\right)} \times \exp(sx)\exp\left(-\frac{x}{\overline{\gamma}}\left(\frac{\Lambda}{|\xi_{11}|^2 - x|\xi_{12}|^2}\right)\right)\mathrm{d}x \tag{59}$$

For the case of $|\xi_{12}|^2 = |\xi_{21}|^2$ and setting $z = |\xi_{11}|^2 - x|\xi_{12}|^2$, equation (59) simplifies to

$$\mathcal{M}_{\gamma_{\mathrm{IQI}}}(s) = C + \frac{s\,C}{|\xi_{12}|^2|\xi_{11}|^2}\exp\left(s\frac{|\xi_{11}|^2}{|\xi_{12}|^2} + \frac{\Lambda}{|\xi_{12}|^2\overline{\gamma}}\right) \times \int_0^{|\xi_{11}|^2} z\exp\left(-z\frac{s}{|\xi_{12}|^2} - \frac{|\xi_{11}|^2\Lambda}{\overline{\gamma}|\xi_{12}|^2 z}\right)\mathrm{d}z \tag{60}$$

which considering the change of variable $y = \frac{zs}{|\xi_{12}|^2}$, is equivalent to (32). On the contrary, for $|\xi_{12}|^2 \neq |\xi_{21}|^2$ and setting $z = |\xi_{11}|^2 - x|\xi_{12}|^2$, equation (59) becomes

$$\mathcal{M}_{\gamma_{\mathrm{IQI}}}(s) = C + \frac{s\,\exp\left(\frac{\Lambda}{|\xi_{12}|^2\overline{\gamma}} + s\frac{|\xi_{11}|^2}{|\xi_{12}|^2}\right)}{|\xi_{12}|^2 - |\xi_{21}|^2} \times \int_0^{|\xi_{11}|^2} \frac{z\,\exp\left(-\frac{|\xi_{11}|^2\Lambda}{|\xi_{12}|^2\overline{\gamma}z} - s\frac{z}{|\xi_{12}|^2}\right)}{\frac{d}{|\xi_{12}|^2-|\xi_{21}|^2} + z}\mathrm{d}z \tag{61}$$

where d is given in (31). For the case of $\left|\frac{|\xi_{11}|^2|\xi_{21}|^2-|\xi_{22}|^2|\xi_{12}|^2}{|\xi_{12}|^2-|\xi_{21}|^2}\right| < |\xi_{11}|^2$, we expand the involved binomial which yields

$$\mathcal{M}_{\gamma_{\mathrm{IQI}}}(s) = C + \sum_{k=0}^{\infty}\frac{(-1)^k\,s\,d^k\exp\left(\frac{\Lambda}{|\xi_{12}|^2\overline{\gamma}} + s\frac{|\xi_{11}|^2}{|\xi_{12}|^2}\right)}{\left(|\xi_{12}|^2 - |\xi_{21}|^2\right)^{k+1}} \times \int_0^{|\xi_{11}|^2} z^{-k}\exp\left(-\frac{|\xi_{11}|^2\Lambda}{|\xi_{12}|^2\overline{\gamma}z} - s\frac{z}{|\xi_{12}|^2}\right)\mathrm{d}z \tag{62}$$

By setting once more $y = xs/|\xi_{12}|^2$, equation (33)) is deduced. Meanwhile for $\left|\frac{|\xi_{11}|^2|\xi_{21}|^2-|\xi_{22}|^2|\xi_{12}|^2}{|\xi_{12}|^2-|\xi_{21}|^2}\right| > |\xi_{11}|^2$, and expanding the binomial in (61), one obtains the following analytic expression

$$\mathcal{M}_{\gamma_{\mathrm{IQI}}}(s) = C + \sum_{k=0}^{\infty}\frac{s\,\exp\left(\frac{\Lambda+s|\xi_{11}|^2\overline{\gamma}}{|\xi_{12}|^2\overline{\gamma}}\right)\left(|\xi_{21}|^2 - |\xi_{12}|^2\right)^k}{d^{k+1}} \times \int_0^{|\xi_{11}|^2} z^{k+1}\exp\left(-\frac{|\xi_{11}|^2\Lambda}{|\xi_{12}|^2\overline{\gamma}z} - s\frac{z}{|\xi_{12}|^2}\right)\mathrm{d}z. \tag{63}$$

Finally, equation (34) is obtained by taking $y = sz/|\xi_{12}|^2$.

REFERENCES

[1] A. Afana, N. Abu-Ali, and S. Ikki, "On the joint impact of hardware and channel imperfections on cognitive spatial modulation MIMO systems: CramerRao bound approach," *IEEE Syst. J.*, vol. 13, no. 2, pp. 1250–1261, June 2019.

[2] S. Mirabbasi and K. Martin, "Classical and modern receiver architectures," *IEEE Commun. Mag.*, vol. 38, no. 11, pp. 132–139, 2000.

[3] S. Bernard, "Digital communications fundamentals and applications," *Prentice Hall, USA*, 2001.

[4] J. Abouei, K. N. Plataniotis, and S. Pasupathy, "Green modulations in energy-constrained wireless sensor networks," *IET commun.*, vol. 5, no. 2, pp. 240–251, 2011.

[5] A. Manolakos, M. Chowdhury, and A. J. Goldsmith, "Constellation design in noncoherent massive SIMO systems," in *IEEE Global Communications Conference*, Austin, Dec 2014, pp. 3690–3695.

[6] B. Natarajan, C. R. Nassar, and S. Shattil, "CI/FSK: bandwidth-efficient multicarrier FSK for high performance, high throughput, and enhanced applicability," *IEEE Trans. Commun.*, vol. 52, no. 3, pp. 362–367, 2004.

[7] F. F. Digham, M. S. Alouini, and S. Arora, "Variable-rate variable-power non-coherent M-FSK scheme for power limited systems," *IEEE Trans. Wireless Commun.*, vol. 5, no. 6, pp. 1306–1312, 2006.

[8] B. Selim, P. C. Sofotasios, S. Muhaidat, and G. K. Karagiannidis, "The effects of I/Q imbalance on wireless communications: A survey," in *IEEE MWSCAS'16*, Abu Dhabi, Oct 2016, pp. 1–4.

[9] S. Park and S. H. Cho, "SEP performance of coherent MPSK over fading channels in the presence of phase/quadrature error and I-Q gain mismatch," *IEEE Trans. Commun.*, vol. 53, no. 7, pp. 1088–1091, 2005.

[10] K. Kiasaleh and T. He, "On the performance of DQPSK communication systems impaired by timing error, mixer imbalance, and frequency nonselective slow rayleigh fading," *IEEE Trans. Veh. Technol.*, vol. 46, no. 3, pp. 642–652, 1997.

[11] B. Selim, P. C. Sofotasios, S. Muhaidat, G. K. Karagiannidis, and B. Sharif, "Performance of differential modulation under RF impairments," in *IEEE International Conference on Communications (ICC)*, Paris, May 2017, pp. 1–6.

[12] B. Selim, S. Muhaidat, P. C. Sofotasios, B. S. Sharif, T. Stouraitis, G. K. Karagiannidis, and N. Al-Dhahir, "Performance analysis of single carrier coherent and noncoherent modulation under i/q imbalance," in *IEEE 87th Vehicular Technology Conference (VTC Spring)*, June 2018, pp. 1–5.

[13] M. Lupupa and J. Qi, "I/Q imbalance in generalized frequency division multiplexing under Weibull fading," in *IEEE PIMRC '15*, Hong Kong, Aug 2015, pp. 471–476.

[14] C. H. Liu, "Performance analysis of two-sided iq imbalance effects in ofdm systems," in *IEEE International Symposium on Personal, Indoor and Mobile Radio Communications*, Tokyo, Sept 2009, pp. 938–942.

[15] M. Windisch and G. Fettweis, "Performance degradation due to I/Q imbalance in multi-carrier direct conversion receivers: A theoretical analysis," in *IEEE International Conference on Communications*, Istanbul, June 2006, pp. 257–262.

[16] Y. Zou, M. Valkama, N. Y. Ermolova, and O. Tirkkonen, "Analytical performance of OFDM radio link under RX I/Q imbalance and frequency-selective rayleigh fading channel," in *IEEE SPAWC'11*, San Francisco, June 2011, pp. 251–255.

[17] F. J. Lopez-Martinez, E. Martos-Naya, J. F. Paris, and J. T. Entrambasaguas, "Exact closed-form BER analysis of OFDM systems in the presence of IQ imbalances and ICSI," *IEEE Trans. Wireless Commun.*, vol. 10, no. 6, pp. 1914–1922, 2011.

[18] A. A. A. Boulogeorgos, P. C. Sofotasios, B. Selim, S. Muhaidat, G. K. Karagiannidis, and M. Valkama, "Effects of RF impairments in communications over cascaded fading channels," *IEEE Trans. Veh. Technol.*, vol. 65, no. 11, pp. 8878–8894, 2016.

[19] B. Selim, S. Muhaidat, P. C. Sofotasios, B. S. Sharif, T. Stouraitis, G. K. Karagiannidis, and N. Al-Dhahir, "Performance analysis of non-orthogonal multiple access under I/Q imbalance," *IEEE Access*, vol. 6, pp. 18 453–18 468, 2018.

[20] ——, "Outage probability of single carrier NOMA systems under I/Q imbalance," in *IEEE Wireless Communications and Networking Conference (WCNC)*, April 2018, pp. 1–6.

[21] ——, "Outage probability of multi-carrier NOMA systems under joint I/Q imbalance," in *International Conference on Advanced Communication Technologies and Networking (CommNet)*, April 2018, pp. 1–7.

[22] B. Selim, S. Muhaidat, P. C. Sofotasios, A. Al-Dweik, B. S. Sharif, and T. Stouraitis, "Radio-frequency front-end impairments: Performance degradation in nonorthogonal multiple access communication systems," *IEEE Veh. Technol. Mag.*, vol. 14, no. 1, pp. 89–97, March 2019.

[23] A. Gouissem, R. Hamila, and M. O. Hasna, "Outage performance of cooperative systems under IQ imbalance," *IEEE Trans. on Commun.*, vol. 62, no. 5, pp. 1480–1489, 2014.

[24] M. Mokhtar, N. Al-Dhahir, and R. Hamila, "OFDM full-duplex DF relaying under I/Q imbalance and loopback self-interference," *IEEE Trans. Vehicular Technol.*, vol. 65, no. 8, pp. 6737–6741, 2016.

[25] L. Samara, M. Mokhtar, O. Ozdemir, R. Hamila, and T. Khattab, "Residual self-interference analysis for full-duplex OFDM transceivers under phase noise and I/Q imbalance," *IEEE Commun. Lett.*, vol. 21, no. 2, pp. 314–317, 2017.

[26] J. Li, M. Matthaiou, and T. Svensson, "I/Q imbalance in AF dual-hop relaying: Performance analysis in Nakagami-m fading," *IEEE Trans. Commun.*, vol. 62, no. 3, pp. 836–847, 2014.

[27] ——, "I/Q imbalance in two-way AF relaying," *IEEE Trans. Commun.*, vol. 62, no. 7, pp. 2271–2285, 2014.

[28] X. Zhang, M. Matthaiou, M. Coldrey, and E. Bjrnson, "Impact of residual transmit RF impairments on training-based MIMO systems," *IEEE Trans. Commun.*, vol. 63, no. 8, pp. 2899–2911, 2015.

[29] N. Kolomvakis, M. Matthaiou, and M. Coldrey, "IQ imbalance in multiuser systems: Channel estimation and compensation," *IEEE Trans. Commun.*, vol. 64, no. 7, pp. 3039–3051, 2016.

[30] J. Qi and S. Aissa, "Analysis and compensation of I/Q imbalance in MIMO transmit-receive diversity systems," *IEEE Trans. on Commun.*, vol. 58, no. 5, pp. 1546–1556, 2010.

[31] T. C. W. Schenk, E. R. Fledderus, and P. F. M. Smulders, "Performance analysis of zero-IF MIMO OFDM transceivers with IQ imbalance," *J. Commun.*, vol. 2, no. 7, pp. 9–19, 2007.

[32] B. Narasimhan, S. Narayanan, H. Minn, and N. Al-Dhahir, "Reduced-complexity baseband compensation of joint Tx/Rx I/Q imbalance in mobile MIMO-OFDM," *IEEE Trans. Wireless Commun.*, vol. 9, no. 5, pp. 1720–1728, 2010.

[33] O. Ozdemir, R. Hamila, and N. Al-Dhahir, "I/Q imbalance in multiple beamforming OFDM transceivers: SINR analysis and digital baseband compensation," *IEEE Trans. Commun.*, vol. 61, no. 5, pp. 1914–1925, 2013.

[34] R. Hamila, O. Ozdemir, and N. Al-Dhahir, "Beamforming OFDM performance under joint phase noise and I/Q imbalance," *IEEE Trans. Vehicular Technol.*, vol. 65, no. 5, pp. 2978–2989, 2016.

[35] A. Mehrabian and A. Zaimbashi, "Spectrum sensing in SIMO cognitive radios under primary user transmitter IQ imbalance," *IEEE Syst. J.*, vol. 13, no. 2, pp. 1210–1218, June 2019.

[36] A. Hakkarainen, J. Werner, K. R. Dandekar, and M. Valkama, "Pre-coded massive MU-MIMO uplink transmission under transceiver I/Q imbalance," in *IEEE Global Communications Conf. Workshops*, Austin, Dec 2014, pp. 320–326.

[37] L. Chen, A. Helmy, G. R. Yue, S. Li, and N. Al-Dhahir, "Performance analysis and compensation of joint TX/RX I/Q imbalance in differential STBC-OFDM," *IEEE Trans. Veh. Technol.*, vol. 66, no. 7, pp. 6184–6200, 2017.

[38] M. K. Simon and M.-S. Alouini, *Digital communication over fading channels*. John Wiley & Sons, 2005.

[39] P. Y. *et al.*, "Single-carrier SM-MIMO: A promising design for broadband large-scale antenna systems," *IEEE Commun. Surveys Tutorials*, vol. 18, no. 3, pp. 1687–1716, February 2016.

[40] L. Anttila, M. Valkama, and M. Renfors, "Frequency-selective i/q mismatch calibration of wideband direct-conversion transmitters," *IEEE Transactions on Circuits and Systems II: Express Briefs*, vol. 55, no. 4, pp. 359–363, April 2008.

[41] B. Narasimhan, D. Wang, S. Narayanan, H. Minn, and N. Al-Dhahir, "Digital compensation of frequency-dependent joint Tx/Rx I/Q imbalance in OFDM systems under high mobility," *IEEE J. Sel. Topics Signal Process.*, vol. 3, no. 3, pp. 405–417, 2009.

[42] T. Schenk, *RF Imperfections in High-Rate Wireless Systems*. Springer, 2008.

[43] M. A. Chaudhry and S. M. Zubair, *On a class of incomplete gamma functions with applications*. CRC press, 2001.

[44] I. S. Gradshteyn and I. M. Ryzhik, *Table of Integrals, Series, and Products*, 6th ed. New York: Academic, 2000.

[45] B. Selim, O. Alhussein, S. Muhaidat, G. K. Karagiannidis, and J. Liang, "Modeling and analysis of wireless channels via the mixture of gaussian distribution," *IEEE Trans. Veh. Technol.*, vol. 65, no. 10, pp. 8309–8321, 2016.

[46] S. M. Alamouti, "A simple transmit diversity technique for wireless communications," *IEEE Journal on Selected Areas in Communications*, vol. 16, no. 8, pp. 1451–1458, Oct 1998.

[47] A. ElSamadouny, A. Gomaa, and N. Al-Dhahir, "A blind likelihood-based approach for OFDM spectrum sensing in the presence of I/Q imbalance," *IEEE Trans. Commun.*, vol. 62, no. 5, pp. 1418–1430, 2014.

Bassant Selim (S15M18) received a Masters degree in communication systems from Pierre et Marie Curie (Paris XI) University, Paris, France, in 2011 and a Ph.D. degree from Khalifa University, Abu Dhabi, United Arab Emirates, in 2017. She is currently a postdoctoral fellow at cole de Technologie Suprieure, Montreal, Canada. Her research interests include wireless communications, radio-frequency impairments, and non-orthogonal multiple access. She is a Member of the IEEE.

Sami Muhaidat (S01M07SM11) received the Ph.D. degree in electrical and computer engineering from the University of Waterloo, Waterloo, ON, Canada, in 2006. From 2007 to 2008, he was an NSERC Post-Doctoral Fellow with the Department of Electrical and Computer Engineering, University of Toronto, ON, Canada. From 2008 to 2012, he was an Assistant Professor with the School of Engineering Science, Simon Fraser University, Burnaby, BC, Canada.

Dr. Muhaidat is currently a Professor with Khalifa University, Abu Dhabi, United Arab Emirates, and a Visiting Professor with the Faculty of Engineering, University of Surrey, Surrey, U.K. He has authored over 150 technical papers on these topics. His research interests include wireless communications, physical-layer security, IoT with emphasis on battery-less devices, and machine learning. He is a member of the Mohammed Bin Rashid Academy of scientists. He was a recipient of several scholarships during his undergraduate and graduate studies and a winner of the 2006 NSERC Postdoctoral Fellowship Competition. Dr. Muhaidat serves as an Area Editor for the IEEE TRANSACTIONS ON COMMUNICATIONS.

Paschalis C. Sofotasios (S07M12SM16) was born in Volos, Greece, in 1978. He received the M.Eng. degree from Newcastle University, U.K., in 2004, the M.Sc. degree from the University of Surrey, U.K., in 2006, and the Ph.D.degree from the University of Leeds, U.K., in 2011. His M.Sc. studies were funded by a scholarship from UK-EPSRC and his Ph.D. studies were sponsored by UK-EPSRC and Pace plc. He has held academic positions at the University of Leeds, U.K., the University of California at Los Angeles, Los Angeles, USA, the Tampere University of Technology, Finland, the Aristotle University of Thessaloniki, Greece, and the Khalifa University of Science and Technology, United Arab Emirates, where he is currently an Assistant Professor. His research interests include broad areas of digital and optical wireless communications including topics on pure mathematics and statistics.

Dr. Sofotasios has been a member and co-chair of the Technical Program Committee of numerous IEEE conferences. He received an Exemplary Reviewer Award from the IEEE Communications Letters in 2012 and from the IEEE Transactions on Communications in 2015 and 2016. He was a co-recipient of the Best Paper Award at ICUFN13. He serves as a regular reviewer for several international journals. He currently serves as an Editor for the IEEE Communications Letters.

Bayan S. Sharif (M92SM01) received the B.Sc. degree from Queens University Belfast, U.K., in 1984, the Ph.D. degree from Ulster University, U.K., in 1988, and the D.Sc. degree from Newcastle University, U.K., in 2013. From 1990 to 2012, he was on the Faculty at Newcastle University, U.K., where he held a number of appointments including a Professor of digital communications, the Head of communications and signal processing research, and the Head of the School of Electrical, Electronic and Computer Engineering.

Dr. Sharif is currently the Dean of the College of Engineering, Khalifa University, Abu Dhabi, United Arab Emirates. His main research interests include digital communications with a focus on wireless receiver structures and optimization of wireless networks. He is a Chartered Engineer and a fellow of the IET, U.K.

Thanos Stouraitis (F07) joined Khalifa University as Professor and Chair of the Electrical Engineering and Computer Science Department in 2015. He is also Professor Emeritus with the University of Patras, where he founded, and directed for 15 years, the International Graduate Program on Signal Processing Systems and Communications, a collaboration of the University of Patras (UP) and other European and American Universities. He served as Director of the Electronics and Computers Division of the UP Electrical and Computer Engineering Department. He served on the National Scientific Board for Mathematics and Informatics of Greece. He was a member of the founding Council of the University of Central Greece. He served on the faculties of Ohio State University, the University of Florida, New York University, and the University of British Columbia. He is an IEEE Fellow for his contributions in digital signal processing architectures and computer arithmetic. He served as President of the IEEE Circuits and Systems Society for 2012-13. Dr. Stouraitis holds a Ph.D. from the University of Florida (for which he received the UF Outstanding Ph.D. Dissertation Award), an MSc. in Electrical Computer Engineering from the University of Cincinnati, an MSc. in Electronic Automation from the University of Athens, Greece, and a BSc. in Physics from the University of Athens, Greece. His current research interests include signal and image processing systems, application-specific processor technology and design, computer arithmetic, and design and architecture of optimal digital systems with emphasis on cryptographic systems. He has authored more than 200 technical papers, as well as, several book chapters and holds one US patent on DSP processor design. He has authored the Univ. of Patras Press book Digital Signal Processing, and co-authored the Marcel Dekker Inc. book Digital Filter Design Software for the IBM PC, and the 2017 Arithmetic Circuits for DSP Applications, book by Wiley-IEEE Press. He has led several DSP processor design projects funded by the European Union, American organizations, and the Greek government and industry, with a total funding totaling more than 3 million EUR.

Dr. Stouraitis has delivered more than 10 keynote speeches at international IEEE conferences. He currently serves as Book Series Editor for the River Publishers Series on Signal, Image and Speech Processing. He served as Editor for the Journal of Circuits, Systems, and Computers, as well as, Associate Editor for IEEE Transactions on Circuits and Systems and IEEE Transactions on VLSI, Editor for the IEEE Interactive Magazines, Editor-at-Large for Marcel Dekker Inc., and as a consultant for various industries. He regularly reviews for the IEEE SP, CS, C, and Education Transactions, for IEE Proceedings E, F, G, and for conferences like IEEE ISCAS, ICASSP, VLSI, SiPS, Computer Arithmetic, Euro DAC etc. He regularly reviews proposals for NSF, the European Commission, and other agencies, and serves as external advisor and examiner for Ph.D. theses in several Universities around the world. He has served as general chair of the IEEE conferences ISSCS 2014, ICECS 2010, CASFEST 2010, ISWPC 2008, ISCAS 2006, SiPS 2005, and ICECS 1996. He serves as Industry Forum Exhibition Chair of GlobeCom 2018. He was the Technical Program Chair of MWSCAS 2016, Eusipco 1998 and ICECS 1999. He has served as Chair or as a member of the Technical Program Committees of a multitude of IEEE Conferences. He has served as Chair of the VLSI Systems and Applications (VSA) Technical Committee and as a member of the DSP and the Multimedia Technical Committees of the IEEE Circuits and Systems Society. He was a chair of the Long-term Strategy and Vision Committee of IEEE CASS. He was a founder, and Chair, of the IEEE Signal Processing chapter in Greece.

Dr. Stouraitis has received several technical awards, including the IEEE Guillemin-Cauer Best Paper Award.

George K. Karagiannidis (M96-SM03-F14) was born in Pithagorion, Samos Island, Greece. He received the University Diploma (5 years) and PhD degree, both in electrical and computer engineering from the University of Patras, in 1987 and 1999, respectively. From 2000 to 2004, he was a Senior Researcher at the Institute for Space Applications and Remote Sensing, National Observatory of Athens, Greece. In June 2004, he joined the faculty of Aristotle University of Thessaloniki, Greece where he is currently Professor in the Electrical Computer Engineering Dept. and Director of Digital Telecommunications Systems and Networks Laboratory. He is also Honorary Professor at South West Jiaotong University, Chengdu, China. His research interests are in the broad area of Digital Communications Systems and Signal processing, with emphasis on Wireless Communications, Optical Wireless Communications, Wireless Power Transfer and Applications, Communications for Biomedical Engineering, Stochastic Processes in Biology and Wireless Security.

Dr. Karagiannidis is the author or co-author of more than 500 technical papers published in scientic journals and presented at international conferences. He is also author of the Greek edition of a book on "Telecommunications Systems" and co-author of the book "Advanced Optical Wireless Communications Systems", Cambridge Publications, 2012. He has been involved as General Chair, Technical Program Chair and member of Technical Program Committees in several IEEE and non-IEEE conferences. In the past, he was Editor in IEEE Transactions on Communications, Senior Editor of IEEE Communications Letters, Editor of the EURASIP Journal of Wireless Communications Networks and several times Guest Editor in IEEE Selected Areas in Communications. From 2012 to 2015 he was the Editor-in Chief of IEEE Communications Letters.

Dr. Karagiannidis is one of the highly-cited authors across all areas of Electrical Engineering, recognized from Clarivate Analytics as Web-of-Science Highly-Cited Researcher in the four consecutive years 2015-2018.

Naofal Al-Dhahir (F07) received the Ph.D. degree in electrical engineering from Stanford University, Stanford, CA, USA. He is an Erik Jonsson Distinguished Professor with University of Texas at Dallas, Richardson, TX, USA. From 1994 to 2003, he was a Principal Member of the technical staff with GE Research and ATT Shannon Laboratory. He is co-inventor of 42 issued US patents and co-author of more than 400 papers.

Dr. Al-Dhahir is the co-recipient of four IEEE Best Paper awards. He is the Editor-in-Chief of IEEE TRANSACTIONS ON COMMUNICATIONS.